hexagon:2611.00142v1

Origin-Centered Möbius Circles, Bernoulli Lemniscates, and Beta–Gamma Dyadic Pairings of the Riemann Zeta Function on the Critical Line

Ryan Hackbarth
hackbarthr16@hanover.edu

November 5, 2026

Abstract

We investigate the complex geometry and Eulerian Beta–Gamma arc-length parameterization of the normalized Dirichlet eta terms $t_n(s) = \frac{1}{1-2^{1-s}} \frac{(-1)^{n-1}}{n^s}$ for $s = a + bi$. Whereas individual terms on the critical line $\mathrm{Re}(s) = \frac{1}{2}$ undergo a nearly sixfold modulus oscillation driven by the Euler prefactor $(1 - 2^{1-s})^{-1}$, the two-term partial sum $S_2(s) = t_1(s) + t_2(s)$ traces an exact Möbius circle for every fixed $a \neq 1$ that is centered at the origin $(0, 0)$ if and only if $\mathrm{Re}(s) = \frac{1}{2}$, where it reduces to a scaled Blaschke factor $\frac{1}{\sqrt{2}} B(z)$ of constant radius $\frac{1}{\sqrt{2}}$. Factoring m^{-s} across odd-even dyadic pairs $P_m(s) = t_m(s) + t_{2m}(s) = m^{-s} S_2(s)$ eliminates prefactor amplitude oscillations entirely, collapsing precessing annular rosettes into concentric origin-centered circles on the critical line with strictly descending radii $\mathcal{R}_m = \frac{1}{\sqrt{2m}}$. Removing all odd-even pairs leaves the complementary multiples-of-4 terms $t_{4k}(s) = k^{-s} t_4(s)$: we prove that on the critical line the anchor term $t_4(\frac{1}{2} + ib)$ traces an exact Lemniscate of Bernoulli with foci at $(0, 0)$ and $(1, 0)$ (uniquely for $\mathrm{Re}(s) = \frac{1}{2}$), pure powers of 2 ($k = 2^r$) trace closed periodic multi-loop rational curves, and non-powers of 2 trace precessing lemniscate rosettes, while the dyadic differences $D_{4m}(s) = t_{4m}(s) - t_{8m}(s) = -4^{-s} P_m(s)$ collapse both families into exact origin-centered circles, partitioning the sequence $\{t_n(s)\}_{n=1}^{\infty}$ termwise and decomposing $\zeta(s)$ via analytic continuation. Finally, we establish a pointwise velocity–modulus duality $\left|\frac{dt_4}{d\theta}\right| = \left|t_2(\frac{1}{2} + ib)\right| = \sqrt{\frac{n}{2}} \left|t_n(\frac{1}{2} + ib)\right|$ ($\theta = b \ln 2$) and a double-angle Blaschke identity $-zB(z) = e^{i2\alpha(b)}$ linking the central polar angle $\alpha(b)$ of $t_4(\frac{1}{2} + ib)$ to its fundamental perimeter $\mathcal{L}(t_4) = \frac{\Gamma(1/4)^2}{2\sqrt{\pi}}$, thereby parameterizing every individual term $t_n(\frac{1}{2} + ib)$ and every concentric dyadic circle on the critical line in terms of the regularized inverse incomplete Beta function $I^{-1}_{q(b)}(\frac{1}{4}, \frac{1}{2})$. As a geometric consequence, critical-line zeros $\zeta(\frac{1}{2} + ib) = 0$ are reframed as values of b where the resultant of the inner concentric circles lands on the antipode $-P_1(\frac{1}{2} + ib)$ of the initial circle of constant radius $\mathcal{R}_1 = \frac{1}{\sqrt{2}} = \frac{\pi}{\Gamma(1/4)\Gamma(3/4)}$.

1 Introduction and Definitions

The Dirichlet eta function $\eta(s)$ provides the standard analytic continuation of the Riemann zeta function $\zeta(s)$ across the critical strip $0 < \mathrm{Re}(s) < 1$ via the Euler factor normalization [2, 9, 10, 14]:

$$\zeta(s) = \frac{\eta(s)}{1 - 2^{1-s}}, \quad \text{where } \eta(s) = \sum_{n=1}^{\infty} \frac{(-1)^{n-1}}{n^s}. \tag{1}$$

To examine the local geometry of this summation in the complex plane $\mathbb{C} \cong \mathbb{R}^2$, we distribute the prefactor into each term, defining the normalized sequence:

$$t_n(s) = \frac{1}{1 - 2^{1-s}} \cdot \frac{(-1)^{n-1}}{n^s}, \quad s = a + bi. \tag{2}$$

For any fixed real part a, treating $b \in \mathbb{R}$ as the curve parameter gives each term an instantaneous modulus:

$$|t_n(a+bi)| = \frac{n^{-a}}{\sqrt{1+4^{1-a}-2^{2-a}\cos(b\ln 2)}}. \tag{3}$$

On the critical line $a = \frac{1}{2}$, this modulus breathes between a periapsis minimum $R_{n,\min} = \frac{\sqrt{2}-1}{\sqrt{n}}$ (when $\cos(b\ln 2) = -1$) and an apoapsis maximum $R_{n,\max} = \frac{\sqrt{2}+1}{\sqrt{n}}$ (when $\cos(b\ln 2) = +1$), spanning a nearly sixfold amplitude variation.

In this paper, we demonstrate that grouping terms into dyadic pairs eliminates this prefactor breathing entirely on the critical line $a = \frac{1}{2}$, collapsing the series into an infinite sequence of exact origin-centered concentric circles. We establish the unique origin-centering of the base-2 Möbius circle $S_2(s)$ on $a = \frac{1}{2}$, prove the dyadic pairing identity for odd-even pairs $P_m(s)$, characterize the exact geometric forms and pairings of the complementary multiples-of-4 subseries, and transition in Section 5 from geometric classification to an analytic synthesis connecting the anchor lemniscate $t_4(\frac{1}{2}+ib)$, Euler's Beta and Gamma integrals, and the concentric dyadic circles of $\zeta(s)$.

2 The Base-2 Anchor: $S_2(s) = t_1(s) + t_2(s)$ and the Critical Line $a = \frac{1}{2}$

For $n = 1$ and $n = 2$, the term frequencies $\ln 1 = 0$ and $\ln 2$ resonate with the prefactor frequency $\ln 2$. Letting $z = e^{-ib\ln 2}$ parametrize the unit circle $|z| = 1$, each individual term is a Möbius transformation [11] of $|z| = 1$:

$$t_1(a+bi) = \frac{1}{1-2^{1-a}z}, \qquad t_2(a+bi) = \frac{-2^{-a}z}{1-2^{1-a}z} = \frac{1}{2} - \frac{1}{2}t_1(a+bi). \tag{4}$$

For any $a \neq 1$, $t_1(a+bi)$ and $t_2(a+bi)$ trace exact circles symmetric across the real axis with centers $C_1(a) = (h_1(a), 0)$, $C_2(a) = (h_2(a), 0)$ and radii $\mathcal{R}_1(a)$, $\mathcal{R}_2(a)$ given by:

$$h_1(a) = \frac{1}{1-4^{1-a}}, \qquad \mathcal{R}_1(a) = \frac{2^{1-a}}{|1-4^{1-a}|}, \tag{5}$$

$$h_2(a) = \frac{-2^{1-2a}}{1-4^{1-a}}, \qquad \mathcal{R}_2(a) = \frac{2^{-a}}{|1-4^{1-a}|}. \tag{6}$$

On the critical line $a = \frac{1}{2}$, let $B(z) = \frac{\sqrt{2}-z}{1-\sqrt{2}z}$ denote the unit-modulus Blaschke factor ($|B(z)| = 1$ for $|z| = 1$) [12]. Then t_1 and t_2 admit the explicit representations:

$$t_1\left(\frac{1}{2}+bi\right) = -1 + \sqrt{2}\,B(z), \quad \text{centered at } C_1 = (-1,0),\ \mathcal{R}_1 = \sqrt{2} \approx 1.4142 \text{ (Figure 1)}, \tag{7}$$

$$t_2\left(\frac{1}{2}+bi\right) = +1 - \frac{1}{\sqrt{2}}\,B(z), \quad \text{centered at } C_2 = (+1,0),\ \mathcal{R}_2 = \frac{1}{\sqrt{2}} \approx 0.7071 \text{ (Figure 2)}. \tag{8}$$

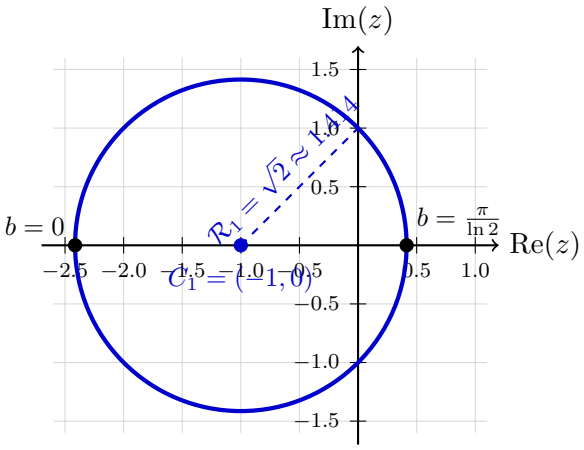


Figure 1: Locus of $t_1(\frac{1}{2}+bi) = \frac{1}{1-2^{1/2-bi}}$ in the complex plane: an exact circle centered at $C_1 = (-1, 0)$ with radius $\mathcal{R}_1 = \sqrt{2} \approx 1.4142$.

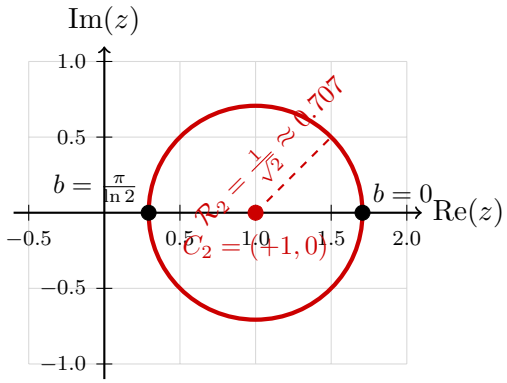


Figure 2: Locus of $t_2(\frac{1}{2}+bi) = \frac{-2^{-(1/2+bi)}}{1-2^{1/2-bi}}$ on the critical line $a = \frac{1}{2}$: an exact circle centered at $C_2 = (+1, 0)$ with radius $\mathcal{R}_2 = \frac{1}{\sqrt{2}} \approx 0.7071$.

Grouping $t_1(s)$ and $t_2(s)$ yields the two-term partial sum:

$$S_2(s) = t_1(s) + t_2(s) = \frac{1-2^{-s}}{1-2^{1-s}} = \frac{1}{2} + \frac{1}{2}t_1(s). \tag{9}$$

Letting $z = e^{-ib\ln 2}$ parametrize the unit circle $|z| = 1$, $S_2(s)$ acts as the Möbius transformation $M_a(z) = \frac{1-2^{-a}z}{1-2^{1-a}z}$.

Proposition 2.1 (Center and Radius of S_2)**.** *For any fixed $a \in \mathbb{R} \setminus \{1\}$, the locus of $S_2(a+bi)$ is a circle centered on the real axis at $C(a) = (h(a), 0)$ with radius $\mathcal{R}(a)$, where:*

$$h(a) = h_1(a) + h_2(a) = \frac{1-2^{1-2a}}{1-4^{1-a}}, \qquad \mathcal{R}(a) = \frac{1}{2}\mathcal{R}_1(a) = \frac{2^{-a}}{|1-4^{1-a}|}. \tag{10}$$

Proof. Since $M_a(z)$ has real coefficients, its real-axis intercepts occur at $z = +1$ ($b = 0$) and $z = -1$ ($b = \frac{\pi}{\ln 2}$):

$$x_+(a) = \frac{1-2^{-a}}{1-2^{1-a}}, \qquad x_-(a) = \frac{1+2^{-a}}{1+2^{1-a}}.$$

The center is the midpoint $h(a) = \frac{x_+(a)+x_-(a)}{2} = \frac{1-2^{1-2a}}{1-4^{1-a}}$, and the radius is the half-width $\mathcal{R}(a) = \frac{|x_+(a)-x_-(a)|}{2} = \frac{|2^{1-a}-2^{-a}|}{|1-4^{1-a}|} = \frac{2^{-a}}{|1-4^{1-a}|}$. □

Theorem 2.2 (Unique Origin-Centering on the Critical Line)**.** *The center of the circle* $S_2(a+bi)$ *lies at the origin* $(0,0)$ *if and only if* $a = \frac{1}{2}$.

Proof. Setting the center $h(a) = 0$ (for $a \neq 1$) requires $1 - 2^{1-2a} = 0$, which yields $1 - 2a = 0 \implies a = \frac{1}{2}$. At $a = \frac{1}{2}$, the centers $C_1 = (-1, 0)$ and $C_2 = (+1, 0)$ cancel, and the map reduces to a scaled Blaschke factor [12]:

$$S_2\left(\frac{1}{2} + bi\right) = \frac{1}{\sqrt{2}}\left(\frac{\sqrt{2} - z}{1 - \sqrt{2}z}\right) = \frac{1}{\sqrt{2}}e^{i\Phi_2(b)}, \tag{11}$$

whose modulus is constant at $\mathcal{R}\left(\frac{1}{2}\right) = \frac{1}{\sqrt{2}}$ for all $b \in \mathbb{R}$ (Figure 3), and whose phase $\Phi_2(b)$ advances with non-uniform angular speed $\left|\frac{d\Phi_2}{db}\right| = \frac{\ln 2}{3-2\sqrt{2}\cos(b\ln 2)}$. □

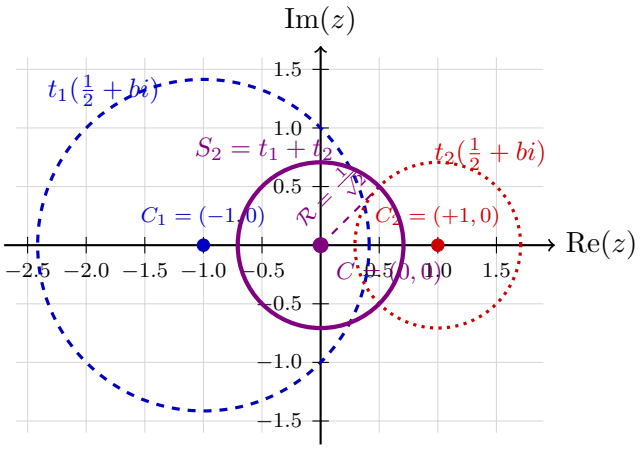


Figure 3: Superposition of $t_1(\frac{1}{2}+bi)$ (dashed blue, $C_1 = (-1,0)$, $\mathcal{R}_1 = \sqrt{2}$), $t_2(\frac{1}{2}+bi)$ (dotted red, $C_2 = (+1,0)$, $\mathcal{R}_2 = \frac{1}{\sqrt{2}}$), and their sum $S_2(\frac{1}{2}+bi) = t_1 + t_2$ (solid purple), which forms an exact circle centered at the origin $C = (0,0)$ with radius $\mathcal{R} = \frac{1}{\sqrt{2}} \approx 0.7071$.

When $a \neq \frac{1}{2}$, the circle $S_2(a+bi)$ immediately shifts its center $C(a) = (h(a), 0)$ off the origin along the real axis, as summarized in Table 1 and illustrated in Figure 4.

Table 1: Center $C(a) = (h(a), 0)$ and radius $\mathcal{R}(a) = \frac{2^{-a}}{|1-4^{1-a}|}$ of $S_2(a+bi) = t_1 + t_2$ across positive values of $a = \mathrm{Re}(s)$.

Real Part a	**Center** $C(a) = (h(a), 0)$	**Radius** $\mathcal{R}(a)$	**Shift Relative to** $(0,0)$
$a = 0.25$ $(0 < a < \frac{1}{2})$	$(\frac{3-\sqrt{2}}{7}, 0) \approx (+0.227, 0)$	$\frac{2^{-1/4}}{2\sqrt{2}-1} \approx 0.460$	Shifted right $(h(a) > 0)$
$a = 0.50$ **(Critical Line)**	$(0, 0)$	$\frac{1}{\sqrt{2}} \approx 0.707$	**Centered at origin** $(0,0)$
$a = 0.75$ $(\frac{1}{2} < a < 1)$	$(-\frac{1}{\sqrt{2}}, 0) \approx (-0.707, 0)$	$\frac{2^{-3/4}}{\sqrt{2}-1} \approx 1.436$	Shifted left $(h(a) < 0)$
$a = 1.50$ $(a > 1)$	$(+\frac{3}{2}, 0) = (+1.500, 0)$	$\frac{1}{\sqrt{2}} \approx 0.707$	Shifted right $(h(a) > 0)$

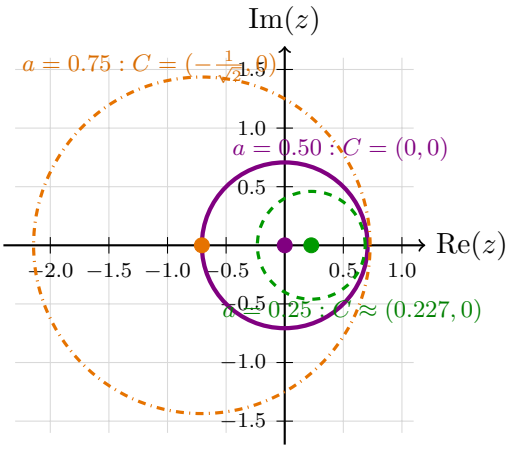


Figure 4: Off-center shift of the circle $S_2(a+bi) = t_1 + t_2$ when $a \neq \frac{1}{2}$: $a = 0.50$ is centered at $(0,0)$ (solid purple, $\mathcal{R} \approx 0.707$), $a = 0.25$ shifts right to $C = (\frac{3-\sqrt{2}}{7}, 0) \approx (+0.227, 0)$ (dashed green, $\mathcal{R} \approx 0.460$), and $a = 0.75$ shifts left to $C = (-\frac{1}{\sqrt{2}}, 0) \approx (-0.707, 0)$ (dash-dot orange, $\mathcal{R} \approx 1.436$).

3 The Dyadic Pairing Identity

For individual unpaired terms $t_n(s) = (-1)^{n-1} n^{-s} t_1(s)$ with $n \geq 3$ ($n \neq 2^k$), the incommensurable rotation $e^{-ib \ln n}$ spins an off-center circle around the origin, sweeping out a thick annular rosette. In contrast, grouping every odd integer $m \in \{1, 3, 5, \dots\}$ with its even double $2m$ locks the prefactor phase to the base-2 term, defining the m-th dyadic pair:

$$P_m(s) = t_m(s) + t_{2m}(s) = \frac{1}{m^s} \left(\frac{1 - 2^{-s}}{1 - 2^{1-s}} \right) = \frac{1}{m^s} S_2(s). \tag{12}$$

Corollary 3.1. *On the critical line $a = \frac{1}{2}$, every dyadic pair $P_m\left(\frac{1}{2} + bi\right)$ traces an exact circle centered at the origin $(0,0)$ with descending radius $\mathcal{R}_m = \frac{1}{\sqrt{2m}}$:*

$$\left| P_m\left(\frac{1}{2} + bi\right) \right| = m^{-1/2} \left| S_2\left(\frac{1}{2} + bi\right) \right| = \frac{1}{\sqrt{m}} \cdot \frac{1}{\sqrt{2}} = \frac{1}{\sqrt{2m}}. \tag{13}$$

For $a \neq \frac{1}{2}$, these circles shift off-center into annular rosettes of thickness $|h(a)| m^{-a}$.

Proof. Direct evaluation from Theorem 2.2 shows that $|S_2(\frac{1}{2} + bi)| = \frac{1}{\sqrt{2}}$ is strictly constant for all $b \in \mathbb{R}$. In particular, beyond $m = 1$ ($P_1 = t_1 + t_2$, $\mathcal{R}_1 = \frac{1}{\sqrt{2}} \approx 0.7071$), the higher odd-even pairs $m = 3$ ($P_3 = t_3 + t_6$, $\mathcal{R}_3 = \frac{1}{\sqrt{6}} \approx 0.4082$) and $m = 5$ ($P_5 = t_5 + t_{10}$, $\mathcal{R}_5 = \frac{1}{\sqrt{10}} \approx 0.3162$) trace exact concentric circles centered at $(0,0)$, as shown in Figure 5. □

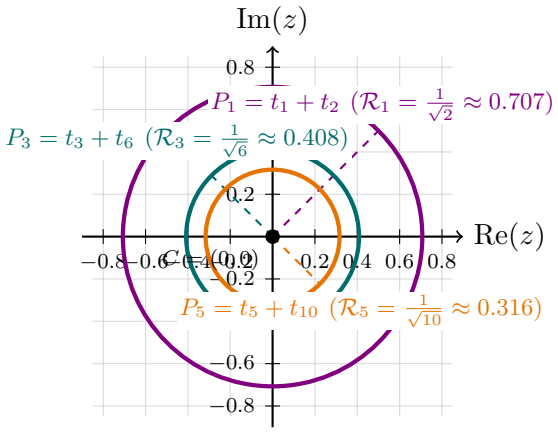


Figure 5: Illustration of Corollary 3.1 on the critical line $a = \frac{1}{2}$: the odd-even pairs $P_1 = t_1 + t_2$ ($\mathcal{R}_1 = \frac{1}{\sqrt{2}} \approx 0.7071$), $P_3 = t_3 + t_6$ ($\mathcal{R}_3 = \frac{1}{\sqrt{6}} \approx 0.4082$), and $P_5 = t_5 + t_{10}$ ($\mathcal{R}_5 = \frac{1}{\sqrt{10}} \approx 0.3162$) trace exact concentric circles centered at the origin $(0, 0)$.

4 Geometric Forms and Dyadic Pairings of the Multiples-of-4 Subseries

When we remove all odd-even dyadic pairs $P_m(s) = t_m(s) + t_{2m}(s)$ ($m = 1, 3, 5, \dots$) from the normalized sequence $\{t_n(s)\}_{n=1}^{\infty}$, we strip out all odd indices ($n \equiv 1, 3 \pmod 4$) and all singly-even indices ($n = 2m \equiv 2 \pmod 4$). The remaining terms are strictly the multiples of 4 ($n = 4k$, $k \in \mathbb{N}$), which factor through the anchor term $t_4(s)$ as:

$$t_{4k}(s) = \frac{-1}{(1 - 2^{1-s})(4k)^s} = \frac{1}{k^s} t_4(s), \qquad t_4(s) = \frac{-4^{-s}}{1 - 2^{1-s}}, \qquad \sum_{k=1}^{\infty} t_{4k}(s) = t_4(s)\, \zeta(s). \tag{14}$$

On the critical line $s = \frac{1}{2} + ib$, where $z = e^{-ib \ln 2}$ parametrizes the unit circle $|z| = 1$, the individual terms $t_{4k}(\frac{1}{2} + ib)$ separate into three distinct geometric forms depending on the index $k \in \mathbb{N}$ (Figure 6).

4.1 The Three Geometric Forms of Individual Terms $t_{4k}(\frac{1}{2} + ib)$

1. **The Anchor Term $t_4(\frac{1}{2} + ib)$ ($k = 1$): An Exact Lemniscate of Bernoulli.** Whereas $t_1(\frac{1}{2} + ib)$ and $t_2(\frac{1}{2} + ib)$ are degree-1 Möbius transformations of $|z| = 1$ and trace exact circles centered at $C_1 = (-1, 0)$ and $C_2 = (+1, 0)$, the anchor term $t_4(\frac{1}{2} + ib) = \frac{-z^2}{2(1-\sqrt{2}z)}$ is quadratic in z. Using the difference of squares $1 - 4^{1-s} = (1 - 2^{1-s})(1 + 2^{1-s})$, $t_4(s)$ decomposes for any $s \in \mathbb{C}$ as:

$$t_4(s) = \frac{1}{4}\left(1 + 2^{1-s}\right) - \frac{1}{4} t_1(s). \tag{15}$$

On the critical line $a = \frac{1}{2}$, substituting $t_1(\frac{1}{2} + ib) = -1 + \sqrt{2}B(z)$ with the unit-modulus Blaschke factor $B(z) = \frac{\sqrt{2}-z}{1-\sqrt{2}z}$ yields the two-arm epicyclic representation:

$$t_4\left(\frac{1}{2} + ib\right) = \frac{1}{2} + \frac{1}{2\sqrt{2}}\Big(z - B(z)\Big). \tag{16}$$

Measuring the distances from $t_4(\frac{1}{2} + ib)$ to the origin $F_1 = (0, 0)$ and to $F_2 = (+1, 0)$ (the center C_2 of t_2) reveals an exact cancellation on $|z| = 1$ (where $\bar{z} = z^{-1}$):

   (a) **Distance to $F_1 = (0, 0)$:** $\left|t_4\left(\frac{1}{2} + ib\right) - 0\right| = \frac{|z|^2}{2|1-\sqrt{2}z|} = \frac{1}{2|1-\sqrt{2}z|}$.

(b) **Distance to $F_2 = (+1, 0)$:** Since $t_4(\frac{1}{2} + ib) - 1 = \frac{-z^2+2\sqrt{2}z-2}{2(1-\sqrt{2}z)} = \frac{-z^2(1-\sqrt{2}\bar{z})^2}{2(1-\sqrt{2}z)}$, its modulus is $\left|t_4\left(\frac{1}{2} + ib\right) - 1\right| = \frac{\left|1-\sqrt{2}z\right|}{2}$.

(c) **Constant Bipolar Product (Lemniscate Law):** Multiplying the two distances eliminates the denominator $\left|1 - \sqrt{2}z\right|$ identically for all $b \in \mathbb{R}$:

$$\left|t_4\left(\frac{1}{2} + ib\right) - 0\right| \cdot \left|t_4\left(\frac{1}{2} + ib\right) - 1\right| = \frac{1}{4}. \tag{17}$$

Consequently, as shown in Figure 6(a), $t_4(\frac{1}{2} + ib)$ traces an exact Lemniscate of Bernoulli with foci $F_1 = (0, 0)$ and $F_2 = (+1, 0)$, central self-intersection node $C_4 = (+\frac{1}{2}, 0)$ (crossed at $\pm 45^\circ$ tangents when $b \ln 2 \equiv \pm\frac{\pi}{4} \pmod{2\pi}$), horizontal span $x \in [\frac{1-\sqrt{2}}{2} \approx -0.2071, \frac{1+\sqrt{2}}{2} \approx +1.2071]$, vertical span $y \in [-\frac{1}{4}, +\frac{1}{4}]$, and Cartesian/polar equations centered at $u = x - \frac{1}{2} = \rho\cos\alpha$, $y = \rho\sin\alpha$:

$$2\left(\left(x - \frac{1}{2}\right)^2 + y^2\right)^2 = \left(x - \frac{1}{2}\right)^2 - y^2 \quad \Longleftrightarrow \quad \rho^2 = \frac{1}{2}\cos(2\alpha). \tag{18}$$

For general $a \neq 1$, a second focus $F_2(a)$ satisfying $|t_4(a + bi)| \cdot |t_4(a + bi) - F_2(a)| = \text{const}$ requires $2^{1-2a} = 4^{1-2a}$, which holds if and only if $a = \frac{1}{2}$—providing a lemniscate counterpart to Theorem 2.2.

2. **Pure Powers of 2 ($4k = 2^{r+2}$, i.e., $k = 2^r \in \{2, 4, 8, \dots\}$): Closed Periodic Multi-Loop Curves.** When $k = 2^r$ $(t_8, t_{16}, t_{32}, \dots)$, the multiplier $k^{-s} = 2^{-r/2}z^r$ is a pure power of $z = e^{-ib\ln 2}$:

$$t_{2^{r+2}}\left(\frac{1}{2} + ib\right) = \frac{-z^{r+2}}{2^{(r+2)/2}\left(1 - \sqrt{2}z\right)}. \tag{19}$$

Because the numerator and denominator share the same fundamental frequency $\ln 2$, these terms are closed rational curves of period $T = \frac{2\pi}{\ln 2} \approx 9.0647$, as shown in Figure 6(b) for $t_8(\frac{1}{2} + ib)$ (2-looped curve) and $t_{16}(\frac{1}{2} + ib)$ (3-looped curve).

3. **Non-Powers of 2 ($k \in \{3, 5, 6, 7, \dots\}$, i.e., $t_{12}, t_{20}, t_{24}, \dots$): Precessing Lemniscate Rosettes.** When k contains an odd prime factor ($k \neq 2^r$), the rotation frequency $\ln k$ in $k^{-s} = \frac{1}{\sqrt{k}}e^{-ib\ln k}$ is incommensurable with $\ln 2$. As shown in Figure 6(c) for $t_{12}(\frac{1}{2} + ib) = 3^{-s}t_4(s)$, each term scales the Anchor Lemniscate $t_4(\frac{1}{2} + ib)$ by $\frac{1}{\sqrt{k}}$ and continuously rotates it around its left focus $F_1 = (0, 0)$ at speed $-b\ln k$, densely filling the origin-centered annulus between $R_{4k,\min} = \frac{\sqrt{2}-1}{2\sqrt{k}}$ and $R_{4k,\max} = \frac{\sqrt{2}+1}{2\sqrt{k}}$.

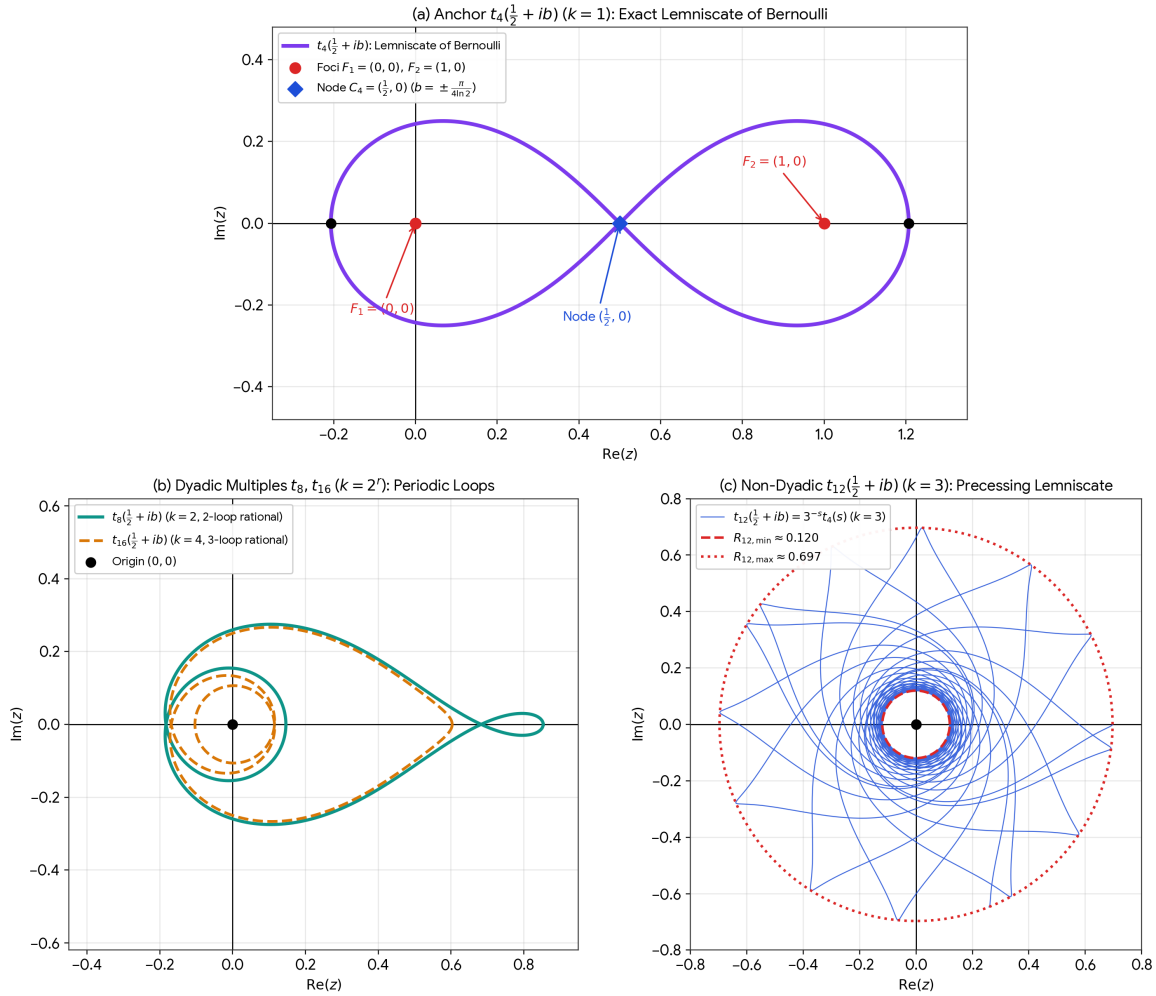


Figure 6: Geometric forms of the individual multiples-of-4 terms $t_{4k}(\frac{1}{2}+ib)$: (a) the Anchor Lemniscate of Bernoulli $t_4(\frac{1}{2}+ib)$ ($k=1$) with foci $F_1=(0,0)$, $F_2=(1,0)$ and self-intersection node $C_4=(\frac{1}{2},0)$; (b) closed periodic multi-loop rational curves t_8, t_{16} for pure powers of 2 ($k=2^r$); and (c) the precessing lemniscate rosette $t_{12}(\frac{1}{2}+ib)=3^{-s}t_4(s)$ ($k=3$) bounded between $R_{12,\min}\approx 0.120$ and $R_{12,\max}\approx 0.697$.

4.2 Producing Origin-Centered Circles from Pure Powers and Non-Powers of 2

Pairing each anchor term with its dyadic double on the critical line $s=\frac{1}{2}+ib$ cancels the $(1-2^{1-s})^{-1}$ prefactor denominator against a $(1-2^{-s})$ numerator, converting non-circular or off-center trajectories into exact origin-centered circles via the Blaschke factor $B(z)=\frac{\sqrt{2}-z}{1-\sqrt{2}z}$ (Figure 7):

1. **First-Level Odd–Even Dyadic Pairs $P_m(s)=t_m(s)+t_{2m}(s)=m^{-s}S_2(s)$ (Figure 7a,b):** In $t_n(s)=\frac{(-1)^{n-1}}{(1-2^{1-s})n^s}$, every odd index m carries sign $+1$ while its even double $2m$ carries sign -1. Thus their direct sum t_m+t_{2m} automatically forms the Blaschke numerator $(1-2^{-s})$. For $m=1$ (pure power of 2, Panel a), adding the off-center circles t_1 ($C_1=(-1,0)$) and t_2 ($C_2=(+1,0)$) cancels their centers to form the origin-centered circle $P_1=S_2$ ($\mathcal{R}_1=\frac{1}{\sqrt{2}}\approx 0.7071$). For $m=3$ (non-power of 2, Panel b), adding the precessing annular rosettes t_3 and t_6 cancels their rotating offsets $\mp 3^{-s}$ at every instant b, collapsing them onto the origin-centered circle P_3 ($\mathcal{R}_3=\frac{1}{\sqrt{6}}\approx 0.4082$).

2. **Multiples-of-4 Dyadic Differences $D_{4m}(s) = t_{4m}(s) - t_{8m}(s) = -4^{-s}P_m(s)$ (Figure 7c,d):** Because every index $4k$ in the multiples-of-4 subseries is even, both $t_{4m}(s)$ and $t_{8m}(s)$ carry the same negative sign $(-1)^{4k-1} = -1$. Consequently, forming the Blaschke numerator $(1 - 2^{-s})$ requires their dyadic difference:

$$D_{4m}(s) = t_{4m}(s) - t_{8m}(s) = -4^{-s}\left(t_m(s) + t_{2m}(s)\right) = -4^{-s}P_m(s). \tag{20}$$

For $k = 1, 2$ (pure powers of 2, Panel c), subtracting the 2-looped curve $t_8(\frac{1}{2} + ib)$ from the Anchor Lemniscate $t_4(\frac{1}{2} + ib)$ yields $t_4 - t_8 = \frac{-z^2}{2\sqrt{2}}B(z)$, an exact origin-centered circle of constant radius $\mathcal{R} = \frac{1}{2\sqrt{2}} \approx 0.3536$. For $k = 3, 6$ (non-powers of 2, Panel d), subtracting the precessing 2-looped rosette $t_{24} = 3^{-s}t_8$ from the precessing lemniscate rosette $t_{12} = 3^{-s}t_4$ eliminates both the lemniscate radius pulsation and the irrational precession, tracing an exact origin-centered circle of constant radius $\mathcal{R} = \frac{1}{2\sqrt{6}} \approx 0.2041$.

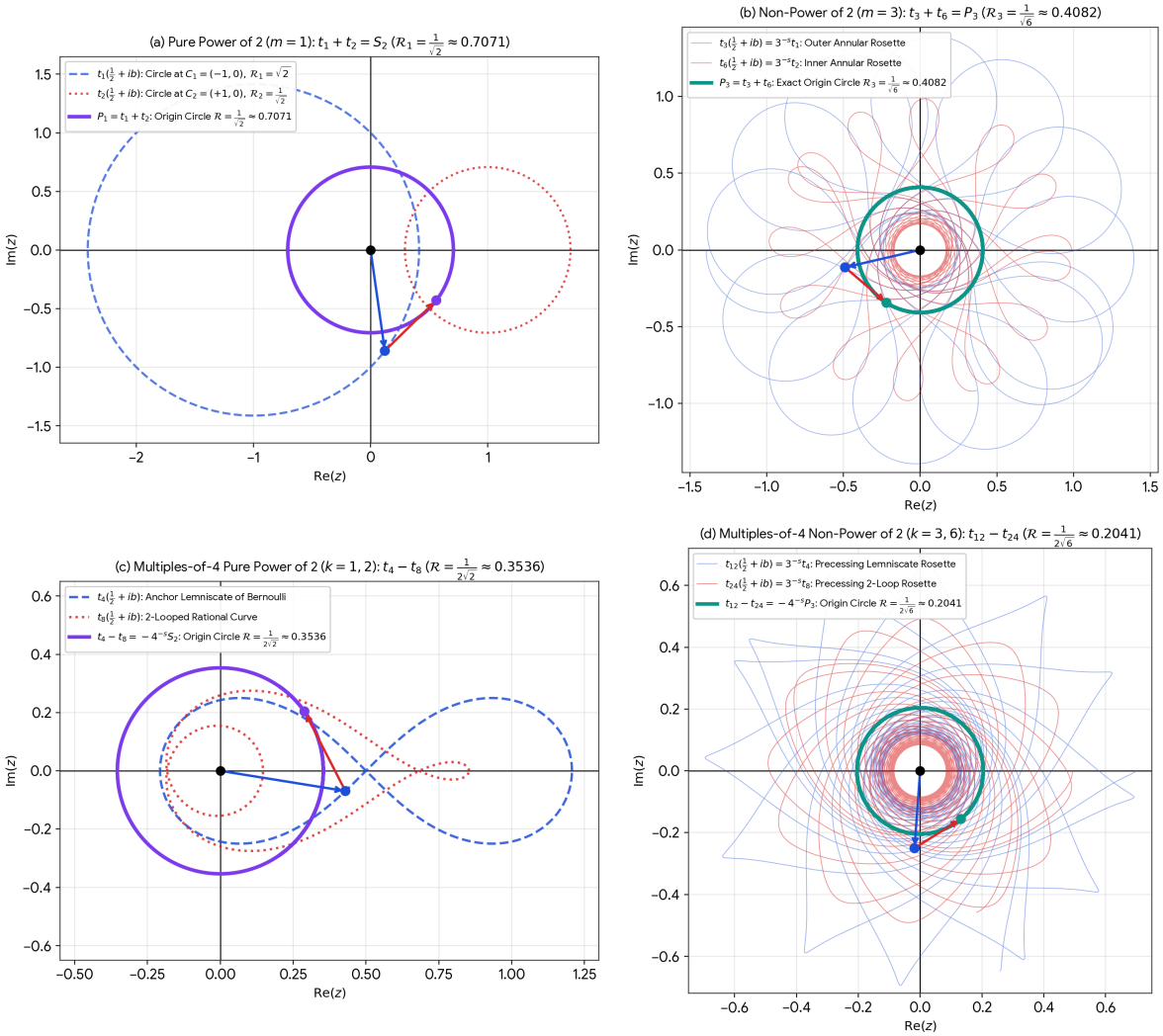


Figure 7: Visual comparison of how dyadic pairing produces exact origin-centered circles on $a = \frac{1}{2}$ for both pure powers of 2 (left column) and non-powers of 2 (right column), with tip-to-tail vectors shown at $b = 1.35$: (a) $t_1 + t_2 = P_1$ ($\mathcal{R}_1 \approx 0.7071$); (b) $t_3 + t_6 = P_3$ ($\mathcal{R}_3 \approx 0.4082$); (c) $t_4 - t_8 = -4^{-s}S_2$ ($\mathcal{R} \approx 0.3536$); and (d) $t_{12} - t_{24} = -4^{-s}P_3$ ($\mathcal{R} \approx 0.2041$).

4.3 Complete Partition of the Series Terms

Every positive integer $n \in \mathbb{N}$ admits a unique factorization $n = 2^r m$ with $m \in \{1, 3, 5, \dots\}$ odd and $r \geq 0$. The odd integers ($r = 0$, 50% of $\mathbb{N}$) and singly-even integers ($r = 1$, 25% of $\mathbb{N}$) form the first-level origin-centered circles $P_m(s) = t_m(s) + t_{2m}(s)$, while the remaining 25% ($r \geq 2$, $n = 4k$) form the multiples-of-4 terms $t_{4k}(s) = k^{-s} t_4(s)$. For $\mathrm{Re}(s) > 1$, where the Dirichlet series converges absolutely, summing the two disjoint subseries yields the exact functional partition:

$$\sum_{n=1}^{\infty} t_n(s) = \sum_{m \text{ odd}} P_m(s) + \sum_{k=1}^{\infty} t_{4k}(s) = \frac{(1-2^{-s})^2}{1-2^{1-s}}\zeta(s) + \frac{-4^{-s}}{1-2^{1-s}}\zeta(s) = \zeta(s). \tag{21}$$

Because the middle and right-hand expressions are meromorphic functions of s across $\mathbb{C}$ (regular for $s \neq 1 + \frac{2\pi i k}{\ln 2}$), this decomposition extends by analytic continuation to the critical strip $0 < \mathrm{Re}(s) < 1$ and specifically to the critical line $\mathrm{Re}(s) = \frac{1}{2}$, while holding term-by-term without rearrangement for every finite partial sum $S_{4N}(s) = \sum_{n=1}^{4N} t_n(s) = \sum_{m<2N \text{ odd}} P_m(s) + \sum_{k=1}^{N} t_{4k}(s) + \sum_{N<m<2N \text{ odd}} t_{2m}(s)$. Re-expanding $\zeta(s)$ in the remainder $t_4(s)\zeta(s)$ recursively decomposes the function into concentric origin-centered circles $P_m(\frac{1}{2} + ib)$ across all dyadic scales $(-4^{-s})^q$ ($q \geq 0$).

5 Connection to the Gamma Function and the Lemniscate Beta–Gamma Arc-Length Parameterization

This section marks a departure from building geometric intuition for the trajectories of individual series terms into a more serious attempt to bridge the analytic connection between the Gamma function, the Lemniscate of Bernoulli, and the Riemann zeta function. Historically, these three pillars of classical analysis did not develop in isolation; their structural unity was forged largely by Leonhard Euler over four decades of eighteenth-century research [1, 2, 3, 4, 5, 6].

The geometric thread began in 1694, when Jacob Bernoulli introduced the *lemniscata* ($\rho^2 = A^2 \cos 2\alpha$) in *Acta Eruditorum* to describe an elastic band and observed that its arc-length integral $\int_0^x \frac{dt}{\sqrt{1-t^4}}$ resisted elementary quadrature, followed in 1718 by Giulio Carlo de' Toschi di Fagnano's discovery that arcs of the lemniscate can nevertheless be algebraically doubled and bisected [6, 7]. In 1729–1730, Euler interpolated the factorial by introducing the integral and infinite-product representations of what is now the Gamma function, alongside binomial integrals of the form $\int_0^1 t^{p-1}(1-t^q)^{r-1}dt$ [1]. Over the next two decades, Euler simultaneously advanced all three subjects: in 1738, while analyzing the rectangular elastica, he discovered that the product of the first and second lemniscate integrals equals $\int_0^1 \frac{dt}{\sqrt{1-t^4}} \cdot \int_0^1 \frac{t^2 dt}{\sqrt{1-t^4}} = \frac{\pi}{4}$ (the integral precursor to the reflection law at $x = \frac{1}{4}$); in 1749, he introduced the alternating eta normalization $\zeta(s) = \frac{\eta(s)}{1-2^{1-s}}$ to continuation-evaluate $\zeta(s)$ across the real axis and formulated the functional relation linking $\zeta(1-s)$ to $\zeta(s)$ through the factorial/Gamma function [2, 5]; and on December 23, 1751—while reviewing Fagnano's *Produzioni Matematiche* for the Berlin Academy—he established the general algebraic addition theorem for lemniscate integrals, founding the theory of elliptic integrals [3, 6].

Euler completed the analytic bridge between binomial integrals and the factorial interpolation in 1771 [4] by proving the reduction of the first-kind Eulerian integral to the second-kind integral—written in Adrien-Marie Legendre's 1811 notation [8] as $B(x,y) = \int_0^1 t^{x-1}(1-t)^{y-1}dt = \frac{\Gamma(x)\Gamma(y)}{\Gamma(x+y)}$. Under the quartic substitution $t = u^{1/4}$, the lemniscate integral reduces directly to $\frac{1}{4}B(\frac{1}{4}, \frac{1}{2}) = \frac{\Gamma(1/4)\Gamma(1/2)}{4\Gamma(3/4)}$, which combines with Euler's reflection formula at $x = \frac{1}{4}$,

$$\Gamma\left(\frac{1}{4}\right)\Gamma\left(\frac{3}{4}\right) = \frac{\pi}{\sin(\pi/4)} = \pi\sqrt{2}, \tag{22}$$

to express the lemniscate constant in closed form as $\varpi = 2\int_0^1 \frac{dt}{\sqrt{1-t^4}} = \frac{\Gamma(1/4)^2}{2\sqrt{2\pi}}$ (whose inverse arc-length function was introduced by Gauss in 1799), while Riemann's 1859 functional equation

$\xi(s) = \frac{1}{2}s(s-1)\pi^{-s/2}\Gamma(\frac{s}{2})\zeta(s) = \xi(1-s)$ evaluates at the real midpoint $s = \frac{1}{2}$ of the critical strip to $\Gamma(\frac{1}{4})$ [10, 9]. In our normalized series $\zeta(s) = \sum_{n=1}^{\infty} t_n(s)$, this classical triad materializes directly on the critical line $\mathrm{Re}(s) = \frac{1}{2}$: the anchor term $t_4(\frac{1}{2} + ib)$ of the remainder subseries $t_4(s)\zeta(s)$ is an exact Lemniscate of Bernoulli whose critical-line semi-axis $A = \frac{1}{\sqrt{2}}$ cancels the $\sqrt{2}$ factor in Euler's reflection identity, allowing both the individual terms $t_n(\frac{1}{2} + ib)$ and the concentric dyadic circles $P_m(\frac{1}{2} + ib)$ and $D_{4m}(\frac{1}{2} + ib)$ to be parameterized explicitly by arc length through Euler's Beta and Gamma functions.

5.1 The Gamma Function and the Exact Arc Length of $t_4(\frac{1}{2} + ib)$

Centered at its self-intersection node $C_4 = (\frac{1}{2}, 0)$, the anchor lemniscate $t_4(\frac{1}{2}+ib) = \frac{1}{2}+\rho(b)e^{i\alpha(b)}$ satisfies the central polar equation $\rho^2 = A^2\cos(2\alpha)$ with semi-axis $A = \frac{1}{\sqrt{2}}$ (matching the radius $\mathcal{R}_1 = \frac{1}{\sqrt{2}}$ of the base-2 Möbius circle $S_2(\frac{1}{2}+ib)$). In central polar coordinates (ρ, α), the arc-length differential along $t_4(\frac{1}{2} + ib)$ is:

$$ds_4 = \sqrt{\rho^2 + \left(\frac{d\rho}{d\alpha}\right)^2}\,|d\alpha| = \frac{A}{\sqrt{\cos(2\alpha)}}\,|d\alpha| = \frac{|d\alpha|}{\sqrt{2\cos(2\alpha)}}. \tag{23}$$

Simultaneously, differentiating $t_4(\frac{1}{2} + ib) = \frac{-z^2}{2(1-\sqrt{2}z)}$ with respect to the base-2 phase $\theta = b\ln 2$ (where $z = e^{-i\theta}$) reveals a pointwise velocity–modulus duality connecting the arc-length speed of t_4 to the breathing modulus $|t_n(\frac{1}{2} + ib)|$ of every term in the series:

$$\frac{dt_4}{d\theta} = \frac{iz^2(2-\sqrt{2}z)}{2(1-\sqrt{2}z)^2} = -iz\,B(z)\,t_2\left(\frac{1}{2}+ib\right) \implies \left|\frac{dt_4}{d\theta}\right| = \left|t_2\left(\frac{1}{2}+ib\right)\right| = \sqrt{\frac{n}{2}}\left|t_n\left(\frac{1}{2}+ib\right)\right|, \tag{24}$$

so that

$$ds_4 = \left|\frac{dt_4}{d\theta}\right| d\theta = \frac{d\theta}{\sqrt{6-4\sqrt{2}\cos\theta}} = \sqrt{\frac{n}{2}}\left|t_n\left(\frac{1}{2}+ib\right)\right| d\theta \qquad (\forall n \in \mathbb{N}). \tag{25}$$

Integrating ds_4 over one complete fundamental period $\theta \in [0, 2\pi]$ ($b \in [0, \frac{2\pi}{\ln 2}]$) traces all four quadrants of the two-loop figure-eight ($\alpha \in [-\frac{\pi}{4}, \frac{\pi}{4}]$ on the right loop and $\alpha \in [\frac{3\pi}{4}, \frac{5\pi}{4}]$ on the left loop). Substituting $2\alpha = \phi$ and applying Euler's Beta integral $B(x,y) = 2\int_0^{\pi/2}(\cos\phi)^{2x-1}(\sin\phi)^{2y-1}d\phi = \frac{\Gamma(x)\Gamma(y)}{\Gamma(x+y)}$ together with the reflection formula $\Gamma(\frac{1}{4})\Gamma(\frac{3}{4}) = \pi\sqrt{2}$ and $\Gamma(\frac{1}{2}) = \sqrt{\pi}$ yields the exact total perimeter $\mathcal{L}(t_4)$ in terms of $\Gamma(\frac{1}{4})$:

$$\mathcal{L}(t_4) = 4\int_0^{\pi/4}\frac{d\alpha}{\sqrt{2\cos(2\alpha)}} = \sqrt{2}\int_0^{\pi/2}(\cos\phi)^{-1/2}\,d\phi = \frac{\sqrt{2}}{2}\,B\left(\frac{1}{4},\frac{1}{2}\right) = \frac{\sqrt{2}\,\Gamma\left(\frac{1}{4}\right)\Gamma\left(\frac{1}{2}\right)}{2\,\Gamma\left(\frac{3}{4}\right)} = \frac{\Gamma\left(\frac{1}{4}\right)^2}{2\sqrt{\pi}} \approx 3.70815. \tag{26}$$

Notice that the semi-axis $A = \frac{1}{\sqrt{2}}$ on the critical line cancels the $\sqrt{2}$ denominator in Gauss's lemniscate constant $\varpi = \frac{\Gamma(1/4)^2}{2\sqrt{2\pi}} \approx 2.62206$, so that $\mathcal{L}(t_4) = \sqrt{2}\varpi = \frac{\Gamma(1/4)^2}{2\Gamma(1/2)}$. Consequently, the quarter-perimeter along a single quadrant from the central node $C_4 = (\frac{1}{2}, 0)$ ($\alpha = \pm\frac{\pi}{4}$) to either horizontal apsis ($\alpha = 0$ or π) is:

$$\mathcal{L}_{\text{quarter}}(t_4) = \frac{\mathcal{L}(t_4)}{4} = \frac{\Gamma\left(\frac{1}{4}\right)^2}{8\sqrt{\pi}} \approx 0.927037, \tag{27}$$

and by Equation (25), the integrated modulus of every individual term $t_n(\frac{1}{2}+ib)$ over one period $\theta \in [0, 2\pi]$ is governed by $\Gamma(\frac{1}{4})$:

$$\int_0^{2\pi}\left|t_n\left(\frac{1}{2}+ib\right)\right| d\theta = \sqrt{\frac{2}{n}}\,\mathcal{L}(t_4) = \frac{\Gamma\left(\frac{1}{4}\right)^2}{\sqrt{2\pi n}} \qquad (\forall n \in \mathbb{N}). \tag{28}$$

5.2 The Lemniscate Beta–Gamma Arc-Length Equation for Individual Terms

To express each individual term $t_n(\frac{1}{2}+ib)$ directly through the Lemniscate Beta–Gamma arc-length integral, let $\tilde{\theta}(b) = \min(b\ln 2 \bmod 2\pi,\, 2\pi - (b\ln 2 \bmod 2\pi)) \in [0,\pi]$ denote the folded base-2 phase, and let $\delta s_4(b)$ denote the arc length along $t_4(\frac{1}{2}+ib)$ measured from the central self-intersection node $C_4 = (\frac{1}{2}, 0)$ (where $\tilde{\theta} = \frac{\pi}{4}$ and $\cos(2\alpha) = 0$) to $\tilde{\theta}(b)$. Substituting $w = \cos^2(2\alpha)$ into Equation (23) (so $dw = -4\cos(2\alpha)\sin(2\alpha)\,d\alpha = -4\sqrt{w(1-w)}\,d\alpha$) transforms $\delta s_4(b)$ into an incomplete Beta integral with parameters $(\frac{1}{4}, \frac{1}{2})$:

$$\delta s_4(b) = \left| \int_{\pi/4}^{\tilde{\theta}(b)} \frac{d\vartheta}{\sqrt{6-4\sqrt{2}\cos\vartheta}} \right| = \frac{1}{4\sqrt{2}} \int_0^{\cos^2(2\alpha(b))} w^{-3/4}(1-w)^{-1/2}\,dw = \frac{\Gamma\left(\frac{1}{4}\right)^2}{8\sqrt{\pi}}\, I_{\cos^2(2\alpha(b))}\left(\frac{1}{4}, \frac{1}{2}\right), \tag{29}$$

where $I_w(x,y) = \frac{1}{B(x,y)}\int_0^w t^{x-1}(1-t)^{y-1}dt$ is the regularized incomplete Beta function. (Equivalently, if $s_4(b)$ is the arc length measured from the nearest horizontal apsis $\tilde{\theta} \in \{0,\pi\}$ to $\tilde{\theta}(b)$, then $\delta s_4(b) = \frac{\Gamma(1/4)^2}{8\sqrt{\pi}} - s_4(b)$.)

Defining the normalized Beta–Gamma arc-length fraction $q(b) \in [0,1]$ by

$$q(b) = \frac{8\sqrt{\pi}\,\delta s_4(b)}{\Gamma\left(\frac{1}{4}\right)^2} = 1 - \frac{8\sqrt{\pi}\,s_4(b)}{\Gamma\left(\frac{1}{4}\right)^2}, \tag{30}$$

and inverting $I_w(\frac{1}{4},\frac{1}{2}) = q(b)$ yields $\cos^2(2\alpha(b)) = I^{-1}_{q(b)}(\frac{1}{4},\frac{1}{2})$, or:

$$\cos\big(2\alpha(b)\big) = \sqrt{I^{-1}_{q(b)}\left(\frac{1}{4},\frac{1}{2}\right)}, \qquad \rho(b) = \frac{1}{\sqrt{2}}\sqrt{\cos\big(2\alpha(b)\big)} = \frac{1}{\sqrt{2}}\left[I^{-1}_{q(b)}\left(\frac{1}{4},\frac{1}{2}\right)\right]^{1/4}. \tag{31}$$

Because every term $t_n(s)$ factors through the anchor lemniscate $t_4(s)$ via $t_n(s) = (-1)^n(\frac{4}{n})^s t_4(s)$, substituting $t_4(\frac{1}{2}+ib) = \frac{1}{2} + \rho(b)e^{i\alpha(b)}$ produces the explicit **Lemniscate Beta–Gamma Arc-Length Equation** for every individual term $t_n(\frac{1}{2}+ib)$ $(n \in \mathbb{N})$:

$$t_n\left(\frac{1}{2}+ib\right) = \frac{(-1)^n}{\sqrt{n}}\, e^{-ib\ln(n/4)}\left[1 + \sqrt{2}\left(I^{-1}_{q(b)}\left(\frac{1}{4},\frac{1}{2}\right)\right)^{1/4} e^{i\alpha(b)}\right], \tag{32}$$

where the quadrant of $\alpha(b)$ is fixed by $\operatorname{sgn}(\cos\alpha(b)) = \operatorname{sgn}(\sqrt{2}\cos(b\ln 2) - 1)$ and $\operatorname{sgn}(\sin\alpha(b)) = \operatorname{sgn}((\sqrt{2}\cos(b\ln 2) - 1)\sin(b\ln 2))$.

5.3 Explicit Beta–Gamma Formulas for Every Concentric Circle

When terms are paired into concentric circles on the critical line $s = \frac{1}{2} + ib$, the Beta–Gamma inversion simplifies even further because the Blaschke factor $B(z) = \frac{\sqrt{2}-z}{1-\sqrt{2}z}$ depends directly on the double angle $2\alpha(b)$ rather than $\alpha(b)$. Specifically, multiplying $B(z)$ by $-z = -e^{-i\theta}$ $(\theta = b\ln 2)$ and rationalizing on $|z| = 1$ gives:

$$-z\,B(z) = \frac{(z-\sqrt{2})^2}{|1-\sqrt{2}z|^2} = \underbrace{\frac{(\sqrt{2}\cos\theta - 1)^2}{3 - 2\sqrt{2}\cos\theta}}_{\cos(2\alpha(b)) \geq 0} + i\,\underbrace{\frac{2\sin\theta\,(\sqrt{2} - \cos\theta)}{3 - 2\sqrt{2}\cos\theta}}_{\sin(2\alpha(b))} = e^{i2\alpha(b)}. \tag{33}$$

Since $\sqrt{2} - \cos\theta > 0$ and $3 - 2\sqrt{2}\cos\theta > 0$ for all $\theta \in \mathbb{R}$, $\cos(2\alpha(b)) \geq 0$ everywhere and $\sin(2\alpha(b))$ carries the exact same sign as $\sin(b\ln 2)$ everywhere. Substituting $\cos^2(2\alpha(b)) = I^{-1}_{q(b)}(\frac{1}{4},\frac{1}{2})$ from Equation (31) gives the universal Lemniscate phase factor:

$$e^{i2\alpha(b)} = \sqrt{I^{-1}_{q(b)}\left(\frac{1}{4},\frac{1}{2}\right)} + i\,\operatorname{sgn}\big(\sin(b\ln 2)\big)\sqrt{1 - I^{-1}_{q(b)}\left(\frac{1}{4},\frac{1}{2}\right)}, \tag{34}$$

and therefore $B(z) = -e^{ib\ln 2}e^{i2\alpha(b)}$. Substituting this relation into $P_m(s) = m^{-s}S_2(s) = \frac{1}{\sqrt{2}}m^{-s}B(z)$ and $D_{4m}(s) = -4^{-s}P_m(s)$ yields explicit Beta–Gamma formulas for every concentric circle in the Riemann zeta series on the critical line:

1. **First-Level Odd–Even Concentric Circles** $P_m = t_m + t_{2m}$ **($m \in \{1,3,5,\dots\}$, Radius** $\mathcal{R}_m = \frac{1}{\sqrt{2m}}$**):**

$$P_m\left(\frac{1}{2}+ib\right) = -\frac{1}{\sqrt{2m}}\,e^{-ib\ln(m/2)}\left[\sqrt{I^{-1}_{q(b)}\left(\frac{1}{4},\frac{1}{2}\right)} + i\ \mathrm{sgn}\big(\sin(b\ln 2)\big)\sqrt{1-I^{-1}_{q(b)}\left(\frac{1}{4},\frac{1}{2}\right)}\right]. \tag{35}$$

2. **Multiples-of-4 Concentric Circles** $D_{4m} = t_{4m} - t_{8m}$ **($m \in \{1,3,5,\dots\}$, Radius** $\mathcal{R}_{4m} = \frac{1}{2\sqrt{2m}}$**):**

$$D_{4m}\left(\frac{1}{2}+ib\right) = +\frac{1}{2\sqrt{2m}}\,e^{-ib\ln(2m)}\left[\sqrt{I^{-1}_{q(b)}\left(\frac{1}{4},\frac{1}{2}\right)} + i\ \mathrm{sgn}\big(\sin(b\ln 2)\big)\sqrt{1-I^{-1}_{q(b)}\left(\frac{1}{4},\frac{1}{2}\right)}\right]. \tag{36}$$

3. **General** r**-th Scale Concentric Circles** $C_{r,m}(s) = (-4^{-s})^r P_m(s)$ **($r \geq 0$, odd** m**, Radius** $\frac{1}{2^r\sqrt{2m}}$**):**

$$C_{r,m}\left(\frac{1}{2}+ib\right) = \frac{(-1)^{r+1}}{2^r\sqrt{2m}}\,e^{-ib\ln(2^{2r-1}m)}\left[\sqrt{I^{-1}_{q(b)}\left(\frac{1}{4},\frac{1}{2}\right)} + i\ \mathrm{sgn}\big(\sin(b\ln 2)\big)\sqrt{1-I^{-1}_{q(b)}\left(\frac{1}{4},\frac{1}{2}\right)}\right]. \tag{37}$$

Figure 8 illustrates the geometry of this correspondence between the normalized lemniscate arc coordinate $q(b)$ on $t_4(\frac{1}{2}+ib)$ (Panel a) and the induced phase $e^{i2\alpha(b)}$ on the concentric dyadic circles P_1, P_3, P_5, and D_4 (Panel b). At the central self-intersection node $C_4 = (\frac{1}{2}, 0)$ ($\tilde{\theta} = \frac{\pi}{4}$), the arc coordinate vanishes ($q = 0$, $I_0^{-1}(\frac{1}{4},\frac{1}{2}) = 0$, $\rho = 0$) and the universal phase factor passes through $e^{i2\alpha} = \pm i$; at the right and left vertices $t_4 = \frac{1\pm\sqrt{2}}{2}$ ($\tilde{\theta} = 0, \pi$), the arc length reaches the full quarter-perimeter $\delta s_4 = \frac{\Gamma(1/4)^2}{8\sqrt{\pi}}$ ($q = 1$, $I_1^{-1}(\frac{1}{4},\frac{1}{2}) = 1$, $\rho = \frac{1}{\sqrt{2}}$) and the universal phase factor aligns with the positive real axis ($e^{i2\alpha} = +1$).

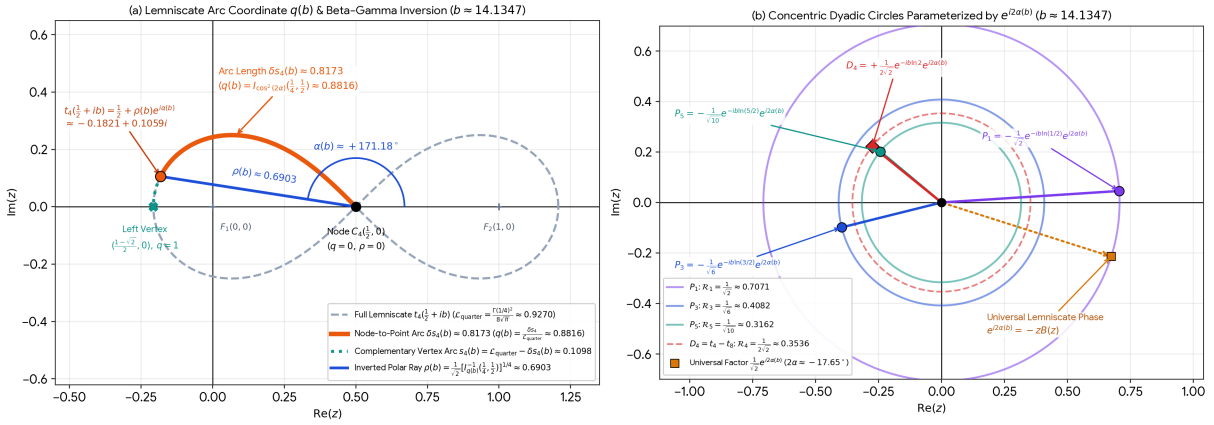


Figure 8: Geometric correspondence between the Lemniscate Beta–Gamma arc-length parameterization and the concentric dyadic circles on the critical line (shown at $b \approx 14.1347$): (a) the arc length $\delta s_4(b)$ measured from the central node $C_4(\frac{1}{2}, 0)$ defines the normalized coordinate $q(b) = \frac{8\sqrt{\pi}\,\delta s_4(b)}{\Gamma(1/4)^2} \in [0, 1]$, whose incomplete Beta inverse $I^{-1}_{q(b)}(\frac{1}{4}, \frac{1}{2}) = \cos^2(2\alpha(b))$ determines the polar ray $(\rho(b), \alpha(b))$ of $t_4(\frac{1}{2} + ib)$; (b) the universal phase factor $e^{i2\alpha(b)} = -zB(z)$ maps $q(b)$ directly onto the concentric circles P_1, P_3, P_5, and D_4.

5.4 Reframing Critical-Line Zeros via the Antipode of the Initial Circle $P_1(\frac{1}{2} + ib)$

When the Euler prefactor $(1 - 2^{1-s})^{-1}$ is retained inside each term $t_n(s)$, isolating the first term $t_1(\frac{1}{2} + ib)$ alone requires the remaining series tail $\sum_{n=2}^{\infty} t_n(\frac{1}{2} + ib)$ at a zero $\zeta(\frac{1}{2} + ib) = 0$ to match a moving target $-t_1(\frac{1}{2} + ib)$ whose modulus breathes nearly sixfold between $\sqrt{2} - 1 \approx 0.4142$ and $\sqrt{2} + 1 \approx 2.4142$. In contrast, isolating the initial origin-centered circle $P_1(s) = S_2(s) = t_1(s) + t_2(s)$ stabilizes the zero target on the critical line $\mathrm{Re}(s) = \frac{1}{2}$ onto a circle of strictly constant radius $\mathcal{R}_1 = \frac{1}{\sqrt{2}} \approx 0.7071$, which simultaneously equals the semi-axis $A = \frac{1}{\sqrt{2}}$ of the anchor Bernoulli lemniscate $t_4(\frac{1}{2} + ib)$ and the Euler reflection ratio at $x = \frac{1}{4}$:

$$\mathcal{R}_1 = A = \frac{1}{\sqrt{2}} = \frac{\pi}{\Gamma\left(\frac{1}{4}\right)\Gamma\left(\frac{3}{4}\right)} = \frac{\varpi}{\mathcal{L}(t_4)}. \tag{38}$$

Combining the odd-index dyadic sums $P_m(s) = t_m(s) + t_{2m}(s)$ ($n = m$ odd) and the even-index dyadic differences $D_{2k}(s) = t_{2k}(s) - t_{4k}(s)$ ($n = 2k$ even, which include the multiples-of-4 circles D_{4m}) into the single concentric circle sequence

$$\mathcal{C}_n(s) = (1 - 2^{-s})t_n(s) = (-1)^{n-1} n^{-s} P_1(s) \qquad (n \in \mathbb{N}) \tag{39}$$

yields an alternating series of origin-centered circles on $\mathrm{Re}(s) = \frac{1}{2}$ with descending radii $\mathcal{R}_n = \frac{1}{\sqrt{2n}}$ that converges conditionally across the critical line to $\sum_{n=1}^{\infty} \mathcal{C}_n(s) = (1 - 2^{-s})\zeta(s)$. Since $|1 - 2^{-1/2-ib}| \geq 1 - \frac{1}{\sqrt{2}} > 0$, a point $b \in \mathbb{R}$ is a critical-line zero of $\zeta(\frac{1}{2} + ib)$ if and only if the resultant of all inner concentric circles $(\mathcal{C}_2, \mathcal{C}_3, \mathcal{C}_4, \dots)$ lands on the exact **antipode** $-P_1(\frac{1}{2} + ib)$ of the initial circle $\mathcal{C}_1 = P_1$:

$$\sum_{n=2}^{\infty} \mathcal{C}_n\left(\frac{1}{2} + ib\right) = -P_1\left(\frac{1}{2} + ib\right) = \frac{1}{\sqrt{2}} e^{ib\ln 2} \left[\sqrt{I^{-1}_{q(b)}\left(\frac{1}{4}, \frac{1}{2}\right)} + i\ \mathrm{sgn}\big(\sin(b\ln 2)\big)\sqrt{1 - I^{-1}_{q(b)}\left(\frac{1}{4}, \frac{1}{2}\right)}\right]. \tag{40}$$

Simultaneously, in the disjoint partition $\zeta(s) = P_1(s) + \sum_{m\geq 3 \text{ odd}} P_m(s) + t_4(s)\zeta(s)$, the multiples-of-4 remainder $t_4(s)\zeta(s)$ vanishes whenever $\zeta(s) = 0$, so the analytic continuation of the odd-even inner circles $\sum_{m\geq 3 \text{ odd}} P_m(\frac{1}{2} + ib)$ and the full series tail $\sum_{n=3}^{\infty} t_n(\frac{1}{2} + ib)$ meet $\sum_{n=2}^{\infty} \mathcal{C}_n(\frac{1}{2} + ib)$ at the exact same antipode $-P_1(\frac{1}{2} + ib)$ on the initial circle of constant radius $\frac{1}{\sqrt{2}}$.

6 Conclusion

By unifying the Dirichlet prefactor with individual series terms, we have shown that the critical line $a = \frac{1}{2}$ is distinguished not only algebraically by functional equation symmetry, but geometrically by two simultaneous characterizations: it is the unique real-axis slice where the base-2 epicyclic anchor $S_2(s)$ and all its odd-even dyadic descendants $P_m(s)$ are centered at the origin $(0, 0)$ [13], and where the complementary multiples-of-4 anchor $t_4(\frac{1}{2} + ib)$ traces an exact Lemniscate of Bernoulli with foci at $(0, 0)$ and $(1, 0)$. Furthermore, the odd-even dyadic sums $t_m + t_{2m} = P_m$ and the multiples-of-4 dyadic differences $t_{4m} - t_{8m} = -4^{-s} P_m$ collapse both periodic multi-loop rational curves and incommensurable precessing rosettes into exact concentric origin-centered circles, accounting for all terms $t_n(s)$ $(n \in \mathbb{N})$. Finally, moving beyond the geometric classification of individual curves, we have shown that the eighteenth-century analytic triad pioneered by Euler—connecting the Lemniscate of Bernoulli, the Beta and Gamma integrals, and the zeta function [1, 2, 3, 4]—converges directly on the critical line: the fundamental perimeter $\mathcal{L}(t_4) = \frac{\Gamma(1/4)^2}{2\sqrt{\pi}}$, the velocity–modulus duality $\left|\frac{dt_4}{d\theta}\right| = \sqrt{\frac{n}{2}} \left|t_n(\frac{1}{2} + ib)\right|$, and the double-angle Blaschke relation $-zB(z) = e^{i2\alpha(b)}$ parameterize both the individual terms $t_n(\frac{1}{2} + ib)$ and the concentric dyadic circles $P_m(\frac{1}{2} + ib)$ and $D_{4m}(\frac{1}{2} + ib)$ through $\Gamma(\frac{1}{4})$ and $I^{-1}_{q(b)}(\frac{1}{4}, \frac{1}{2})$, and reframing critical-line zeros geometrically as points where the inner concentric circles land on the antipode $-P_1(\frac{1}{2} + ib)$ of the initial circle of constant radius $\frac{1}{\sqrt{2}}$, thereby uniting the visual geometry and classical analysis of the Riemann zeta function on the critical line.

Acknowledgments

The author gratefully acknowledges https://tacoyaci.github.io/ for her informal notes and helpful feedback on an earlier version of this manuscript, and thanks Andreas Holmstrom of PeakMath for his encouragement and kind words.

References

[1] L. Euler, "De progressionibus transcendentibus seu quarum termini generales algebraice dari nequeunt," *Commentarii Academiae Scientiarum Imperialis Petropolitanae*, vol. 5, pp. 36–57, 1730 (published 1738); reprinted in *Opera Omnia*, Series 1, vol. 14, pp. 1–24.

[2] L. Euler, "Remarques sur un beau rapport entre les séries des puissances tant directes que réciproques," *Mémoires de l'Académie des Sciences de Berlin*, vol. 17, pp. 83–106, 1768 (read 1749); reprinted in *Opera Omnia*, Series 1, vol. 15, pp. 70–90.

[3] L. Euler, "Observationes de comparatione arcuum curvarum irrectificabilium," *Novi Commentarii Academiae Scientiarum Imperialis Petropolitanae*, vol. 6, pp. 58–84, 1761 (read 1751); reprinted in *Opera Omnia*, Series 1, vol. 20, pp. 80–107.

[4] L. Euler, "Evolutio formulae integralis integratione a valore $x = 0$ ad $x = 1$ extensa," *Novi Commentarii Academiae Scientiarum Imperialis Petropolitanae*, vol. 16, pp. 91–139, 1772 (read 1771); reprinted in *Opera Omnia*, Series 1, vol. 17, pp. 316–357.

[5] R. Ayoub, "Euler and the Zeta Function," *The American Mathematical Monthly*, vol. 81, no. 10, pp. 1067–1086, 1974.

[6] R. Ayoub, "The Lemniscate and Fagnano's Contributions to Elliptic Integrals," *Archive for History of Exact Sciences*, vol. 29, no. 2, pp. 131–149, 1984.

[7] J. Stillwell, *Mathematics and Its History*, 3rd ed., Undergraduate Texts in Mathematics, Springer, New York, 2010.

[8] E. T. Whittaker and G. N. Watson, *A Course of Modern Analysis*, 4th ed., Cambridge University Press, Cambridge, 1927.

[9] E. C. Titchmarsh and D. R. Heath-Brown, *The Theory of the Riemann Zeta-Function*, 2nd ed., Oxford University Press, 1986.

[10] H. M. Edwards, *Riemann's Zeta Function*, Academic Press, New York, 1974.

[11] T. Needham, *Visual Complex Analysis*, Oxford University Press, 1997.

[12] J. B. Garnett, *Bounded Analytic Functions*, Revised 1st ed., Graduate Texts in Mathematics, vol. 236, Springer, 2007.

[13] H. Bohr and R. Courant, "Neue Anwendungen der Theorie der Diophantischen Approximationen auf die Riemannsche Zetafunktion," *Journal für die reine und angewandte Mathematik*, vol. 144, pp. 249–274, 1914.

[14] T. M. Apostol, *Introduction to Analytic Number Theory*, Undergraduate Texts in Mathematics, Springer-Verlag, 1976.